Control of a dynamic load emulator for hardware-in-the-loop testing of fluidic artificial muscle bundles

Mazzoleni, Nicholas, Kim, Jeong Yong, Bryant, Matthew

Nicholas Mazzoleni, Jeong Yong Kim, Matthew Bryant, "Control of a dynamic load emulator for hardware-in-the-loop testing of fluidic artificial muscle bundles," Proc. SPIE 12041, Bioinspiration, Biomimetics, and Bioreplication XII, 1204106 (20 April 2022); doi: 10.1117/12.2612920

SPIE.

Event: SPIE Smart Structures + Nondestructive Evaluation, 2022, Long Beach, California, United States

Control of a dynamic load emulator for hardware-in-the-loop testing of fluidic artificial muscle bundles

Nicholas Mazzoleni[a], Jeong Yong Kim[a], Matthew Bryant[a]
[a]North Carolina State University Department of Mechanical & Aerospace Engineering,
1840 Entrepreneur Dr., Raleigh, NC 27606

ABSTRACT

Fluidic artificial muscles (FAMs) have emerged as a viable and popular robotic actuation technique due to their low cost, compliant nature, and high force-to-weight-ratio. In recent years, the concept of variable recruitment has emerged as a way to improve the efficiency of conventional hydraulic robotic systems. In variable recruitment, groups of FAMs are bundled together and divided into individual motor units. Each motor unit can be activated independently, which is similar to the sequential activation pattern observed in mammalian muscle. Previous researchers have performed quasistatic characterizations of variable recruitment bundles and some simple dynamic analyses and experiments with a simple 1-DOF robot arm. We have developed a linear hydraulic characterization testing platform that will allow for the testing of different types of variable recruitment bundle configurations under different loading conditions. The platform consists of a hydraulic drive cylinder that acts as a cyber-physical hardware-in-the-loop dynamic loading emulator and interfaces with the variable recruitment bundle. The desired inertial, damping and stiffness properties of the emulator can be prescribed and achieved through an admittance controller. In this paper, we test the ability of this admittance controller to emulate different inertial, stiffness, and damping properties in simulation and demonstrate that it can be used in hardware through a proof-of-concept experiment. The primary goal of this work is to develop a unique testing setup that will allow for the testing of different FAM configurations, controllers, or subsystems and their responses to different dynamic loads before they are implemented on more complex robotic systems.

Keywords: Fluidic artificial muscles, hardware-in-the-loop, load emulator, cyber-physical system, bioinspired robotics

1. INTRODUCTION

1.1 Brief overview of hardware-in-the-loop (HIL) testing

Hardware-in-the-loop (HIL) testing is an effective way to rapidly prototype engineering designs by allowing for the observation of how a specific piece of hardware interacts with its environment. Hardware-environment interactions can be unidirectional or bidirectional, depending on the application. For example, if we want to test how a vehicle chassis and suspension system responds to a given road profile, we might simulate this road profile's effect on a physical prototype of the chassis and suspension components using a combination of sensing and actuation in a test lab.[1] In such a system, the coupling between the physical system and the simulated system is unidirectional because the physical hardware response (e.g. the motion of the chassis and suspension prototype) to the simulated system (e.g. from the simulated road) has no influence on the simulated system. In other systems, the coupling between the physical and simulated systems is bidirectional since energy is exchanged in both directions. A system that captures this bidirectionality is called a closed-loop HIL emulator.[1] One common system that uses HIL emulators is an electric drive system, where the hardware under test is the power electronics and electric machine, and the simulated system is the mechanical load behavior.[2] Another common system is a vehicle, where the hardware under test is an engine and the simulated system is the rest of the vehicle/driver behavior (this is called "engine-in-the-loop" testing).[1] The construction of an effective HIL emulator requires the necessary physical hardware (which includes sensors and actuators), a high-fidelity model of the emulated environment, and the proper control architecture to integrate the two together. If this can be achieved, HIL emulators are a powerful way to test hardware in a quick, cost-effective, repeatable and non-destructive manner.[1]

Bidirectional closed-loop HIL controlled systems can be either impedance-controlled, where they receive motion as a control input and send force as a control output, or they can be admittance controlled, where they receive force as a control input and send motion as a control output. Recently, HIL testing has been used in fluid-structure interaction experiments as a way to determine how structures with different inertial, stiffness, and damping properties interact with the fluid forces

Bioinspiration, Biomimetics, and Bioreplication XII, edited by Raúl J. Martín-Palma
Mato Knez, Akhlesh Lakhtakia, Proc. of SPIE Vol. 12041, 1204106
© 2022 SPIE · 0277-786X · doi: 10.1117/12.2612920

acting on them.[3,4] This type of HIL emulation, which is admittance-based, is called cyber-physical fluid dynamics (CPFD). This is a more complicated class of HIL emulator, because unlike the emulator used to test electric drives,[2] which emulates the response of a physical system completely in simulation, these CPFD emulators use actual hardware (typically a linear actuator) to emulate the inertial and stiffness properties of the structure they are trying to control. In this paper, we will develop a similar type of emulator, but instead of studying fluid-structure interaction, we will be studying how bio-inspired fluidic artificial muscle architectures interact with their environment.

1.2 Bioinspired FAM actuation strategies motivate HIL emulator development

Fluidic artificial muscles (FAMs), also known as McKibben muscles, were invented by Joseph McKibben in the 1960s with the original purpose of assisting polio victims.[5] These actuators consist of an elastomeric bladder surrounded by a braided sheath. When the elastomeric bladder is pressurized pneumatically or hydraulically, it radially expands, and the kinematic constraints imposed by the braid cause it to axially contract. Although the mechanism by which FAMs are actuated is dissimilar to that of biological muscles, the soft and compliant nature of FAMs, along with their contractile muscle-like behavior, high force-to-weight ratio, and low cost make them a popular actuator choice within the bioinspired robotics community. Numerous robotic exoskeletons and rehabilitative devices have been constructed using FAMs that act much like biological muscles, typically operating in antagonistic pairs to achieve bi-directional motion of robotic joints.[6,7] In recent years, FAMs have been used in a new bio-inspired actuation strategy called variable recruitment. First developed by Bryant et al.[8], variable recruitment places FAMs in a bundle and divides them into separate motor units (MUs) that can be actuated independently and sequentially. This is inspired by a biological principle known as Henneman's Size Principle, which states that mammalian muscles consist of thousands of individual fibers divided into motor units that are activated in order from smallest to largest, depending on the load required.[9] In traditional hydraulic robotic systems, an actuator (typically a hydraulic piston-cylinder) needs to be sized such that it can provide the largest load required by a given application, even if this load is only required for a small fraction of its operation. Because of this, for any loads lower than the maximum load, the system has to throttle to a lower pressure, resulting in energy losses. In variable recruitment bundles, due to the discrete nature of the individual motor units, when lower loads are needed, the bundle can operate in a lower recruitment state at a pressure much closer to source pressure. This results in less lost energy and significant gains in efficiency, which has been shown in several studies, along with bandwidth improvements.[8,10–12]

Variable recruitment control schemes have been developed by both Jenkins et al.[11] and Meller et al.[12], and Meller et al. experimentally demonstrated efficiency gains on a 1-DOF robot arm actuated by a variable recruitment bundle with 3 MUs consisting of 2 FAMs each. Efficiency gains from variable recruitment were also demonstrated using a custom linear hydraulic actuation characterization device, or linear dynamometer for short, first developed by Chipka et al.[13]. This device consists of a double-acting hydraulic cylinder (TRD Manufacturing MH series, 2.5-inch bore, 1-inch rod diameter) controlled by a MOOG G761 servovalve that serves as a drive actuator, and has three separate MOOG G761 servovalves for FAM bundle actuation, making it possible for bundles under test to have three separate recruitment states. The force of the FAMs acting on the cylinder are measured with an inline load cell (Transducer Techniques SSM-1K) and the position of the cylinder is measured using an LVDT position sensor (RDP Group ACT series).

Until now, the linear dynamometer has only been used to prescribe a predetermined position trajectory to the drive cylinder (using the LVDT as position feedback) while simultaneously prescribing a predetermined force trajectory to the variable recruitment bundle and using the load cell to serve as feedback for active pressure control of the FAMs. While this method of testing can be used to obtain valuable information regarding the efficiency benefits of variable recruitment for a specific system, it is limited in scope since there is no actual coupling between the drive cylinder and the FAM bundle. This means that the behavior of the FAM bundle and the drive cylinder have very little effect on each other. A much more integrated (but complicated) approach would be to use the drive cylinder to emulate the inertial and stiffness properties of a given load. This approach would allow for variable recruitment strategies and control schemes for different robotic limbs and applications to be tested without having to construct the robots themselves. Instead, the drive cylinder could be programmed to behave with the inertial properties of a desired robotic system and would thus respond to FAM force inputs accordingly. This would allow for much more rapid prototyping and design refinement and would help bridge the gap between modeling and experiments in the FAM and variable recruitment literature.

1.3 Outline of contributions in this paper

In this paper, we will analytically demonstrate that the linear dynamometer can be used as a HIL emulator to emulate the dynamics of a desired structure. We will start by developing a model for the hydraulic drive cylinder and analytically

demonstrating the HIL emulator with a simple mass-spring-damper system. We will then demonstrate the HIL emulator in hardware through a proof-of-concept experiment.

2. DYNAMIC MODELING OF DRIVE CYLINDER

2.1 Hydraulic drive cylinder modeling

In order to perform a proper analytical demonstration of the hydraulic drive cylinder as a HIL emulator, it is necessary to develop a physics-based model for it. The hydraulic drive cylinder used for the linear dynamometer can be modeled using techniques from both Ruderman et al.[14] and Jelali and Kroll.[15] It is worth noting that to develop this model, we assume that a hydraulic pump supplies constant pressure to the cylinder, the pressure within the reservoir is constant, and that pipeline dynamics and effects are negligible.

We begin with the conservation of mass for a control volume:

$$\sum \dot{m}_{in} - \sum \dot{m}_{out} = \frac{d(\rho V)}{dt} = \rho \dot{V} + \dot{\rho} V \tag{1}$$

where $\dot{m}_{in}$ is the mass flow rate into the control volume, $\dot{m}_{out}$ is the mass flow rate out of the control volume, ρ is the density of the hydraulic fluid, and V is the volume of the hydraulic fluid. Dividing both sides by the density of the hydraulic fluid, we obtain the following:

$$\sum Q_{in} - \sum Q_{out} = \dot{V} + \frac{V}{E}\dot{\rho} \tag{2}$$

where Q_{in} and Q_{out} are the volumetric flow rates in and out of the control volume and E is the bulk modulus of the hydraulic fluid. These equations can be applied to the hydraulic cylinder shown in Figure 1.

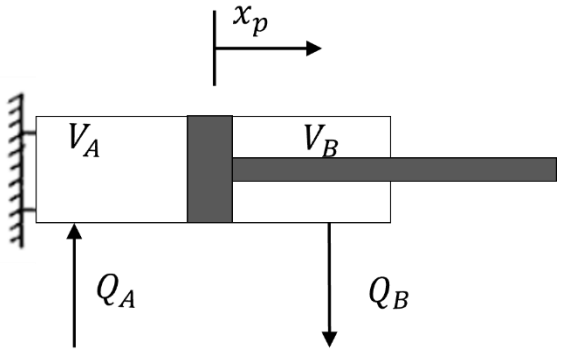

Figure 1. Schematic of double-acting hydraulic cylinder used in linear dynamometer with important variables labeled.

For cylinder chamber A, the conservation of volumetric flow rate can be applied as follows:

$$Q_A = A_A \dot{x}_p + \frac{V_A}{E}\dot{P}_A \tag{3}$$

where A_A is the cross-sectional area of the A side of the piston. The time rate of change of the volume of fluid in chamber A is given by:

$$\dot{V}_A = A_A \dot{x}_p \tag{4}$$

So, the equation can be re-arranged to be an ODE describing the pressure dynamics of the fluid in chamber A:

$$\dot{P}_A = \frac{E}{V_A}\left[Q_A - A_A \dot{x}_p\right] \tag{5}$$

In a similar way, the pressure dynamics of the fluid in chamber B can be written as:

$$\dot{P}_B = \frac{E}{V_B}\left[Q_B + A_B \dot{x}_p\right] \tag{6}$$

where A_B is the cross-sectional area of the B side of the piston. The expressions for the volume in both cylinder chambers are given by:

$$V_A = V_{A0} + A_A x_p \tag{7}$$

$$V_B = V_{B0} + A_B x_p \tag{8}$$

The chamber flows Q_A and Q_B can be calculated by using the equations for flow rate of a two-stage servovalve:[15]

$$Q_A = \begin{cases} u_v c_v \sqrt{P_S - P_A}, u_v > 0 \\ u_v c_v \sqrt{P_A - P_T}, u_v < 0 \\ 0, u_v = 0 \end{cases} \tag{9}$$

$$Q_B = \begin{cases} -u_v c_v \sqrt{P_B - P_T}, u_v > 0 \\ -u_v c_v \sqrt{P_S - P_B}, u_v < 0 \\ 0, u_v = 0 \end{cases} \tag{10}$$

where u_v is the valve voltage input, c_v is the valve constant, P_S is the supply pressure, and P_T is the reservoir pressure. The valve coefficient c_v was determined using data collected by Meller et al. for a MOOG G761 two-stage servovalve.[16]

The actual dynamics of the piston-cylinder can be given by this simple second-order ODE:

$$m_p \ddot{x}_p = P_A A_A - P_B A_B - F_f - F_L \tag{11}$$

where F_f and F_L are the frictional force and the load force acting on the cylinder. These differential equations can be implemented in Simulink and the position of the cylinder can be controlled using simple PID control. This position control will be used in the following sections of the paper in order to show the ability of the cylinder to emulate the dynamics of a desired system.

3. CASE STUDY: USING HARDWARE-IN-THE-LOOP EMULATOR AS MASS-SPRING-DAMPER

As a baseline proof-of-concept, we will start by showing that the hydraulic drive cylinder can be used to emulate a mass-spring damper. Let us begin by considering a diagram of the actual hardware setup and the desired hardware setup we wish to emulate:

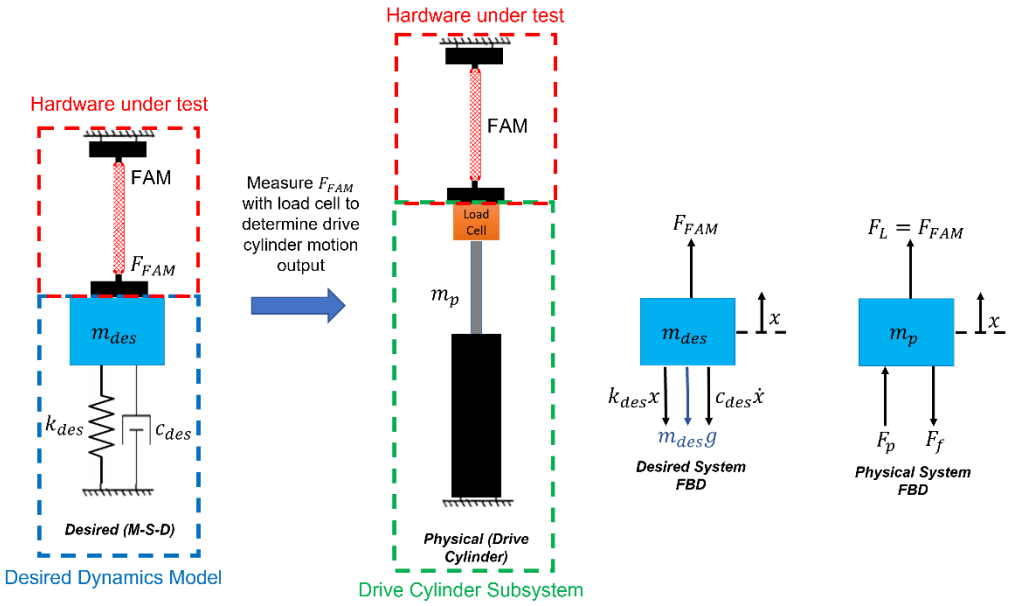

Figure 2. From left to right, this figure shows the actual system (piston-cylinder attached to FAM, with load cell at interface between the two), the desired system (mass-spring-damper attached to FAM), and the free-body diagrams associated with both of these systems.

The actual hardware setup consists of a FAM attached to the hydraulic drive cylinder. At the interface between the FAM and drive cylinder, there is a load cell and a position sensor for feedback control. In the desired hardware setup, the drive cylinder is replaced by a mass-spring-damper. Based on the desired hardware setup we wish to emulate, the equation of motion of the desired system can be written as follows:

$$m_{des}\ddot{x} + c_{des}\dot{x} + k_{des}x = F_{FAM} - m_{des}g \tag{12}$$

where m_{des}, k_{des}, and c_{des} are the desired mass, stiffness and damping terms and F_{FAM} is the force exerted by the FAM. The FAM model used to calculate the FAM force was developed by Meller et al.[17] and used by Jenkins et al.[11] This model modifies the ideal model to account for pressure-dependent free strain by using empirically determined correction factors. This model is given by:

$$F_{mod} = \kappa_f \pi r_0^2 P_a (a(1 - \kappa_\varepsilon \varepsilon)^2 - b) \tag{13}$$

where κ_f is the empirical force correction factor, κ_ε is the empirical strain correction factor, r_0 is the outer radius of the FAM, a and b are braid angle-based parameters found in the ideal model[5], P_a is applied pressure to FAM, and ε is the strain of the FAM. The empirical factors in this FAM model are based on experimental curve fits of blocked force and free strain up to a maximum pressure of 7 bars. For the FAM in this study, we will use curve-fits obtained by Meller et al.[17] for a latex bladder material:

$$\varepsilon_{fit}(P_a) = 1.242 \times 10^{-18} P_a^3 - 2.167 \times 10^{-12} P_a^2 + 1.342 \times 10^{-6} P_a - 0.0377 \tag{14}$$

$$F_{fit}(P_a) = 6.239 \times 10^{-4} P_a - 3.479 \quad (15)$$

The FAM parameters and the desired system parameters used for this case study are shown below in Table 1. The simulation consists of three test cases. In each test case, the mass and stiffness parameters are kept the same but different damping ratios of 1, 2, and 5 are used. Typically, such high damping ratios would result in an extremely overdamped mass-spring damper system. However, in this system, since there is a FAM coupled with the mass-spring-damper, there is an implicit FAM stiffness within the system that lowers the overall system damping, resulting in an "apparent" damping ratio. This will be more clearly demonstrated in the simulation results.

Table 1. FAM parameters and desired system parameters used in simulation.

FAM Parameter	**Value**	**Desired system parameters**	**Simulation 1**	**Simulation 2**	**Simulation 3**
Unpressurized length (m)	0.127	m_{des} (kg)	5	6	7
Unpressurized radius (m)	0.00635	k_{des} (N/m)	125	150	175
Unpressurized braid angle (deg)	28.7	ζ_1	5	5	5
Maximum free strain	0.2611	ζ_2	2	2	2
		ζ_3	1	1	1

For our analysis, we will consider the loading scenario in which a constant pressure input of 206.84 kPa (30 psi) is applied to the FAM. When pressurized, the FAM exerts a force on the hydraulic cylinder. The load cell attached to the cylinder measures the force exerted by the FAM, and this force measurement is used, in coordination with the desired system and its parameters, to determine how much the cylinder needs to move in response to this force input to properly emulate the desired system dynamics. A basic block diagram of this process is shown below.

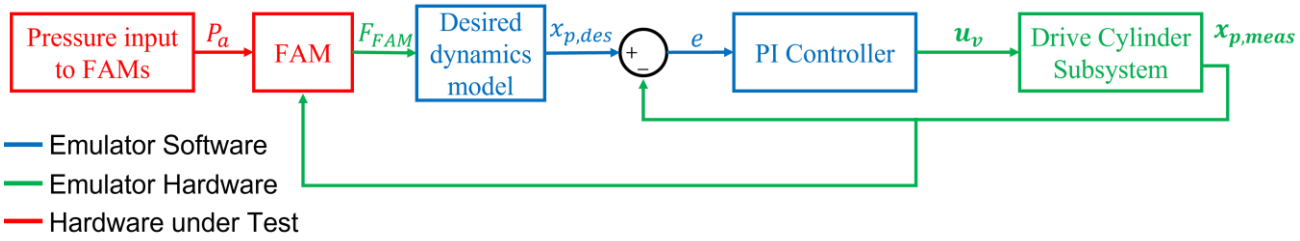

Figure 3. Block diagram demonstrating the admittance control algorithm used to emulate the dynamics of a desired structure.

Not all the parameters for the actual hydraulic drive cylinder shown in Figure 1 are known (especially the friction parameters), so instead, the parameters used in Ruderman et al.[14] will be used for the drive cylinder subsystem. This will serve as a sufficient proof-of-concept of the idea presented in this paper. In future work, we plan to determine the relevant parameters for our own hardware to provide more accurate simulations of the experimental setup and hardware. A simple PI controller is used to control the position of the hydraulic drive cylinder. The results of both simulations are shown below.

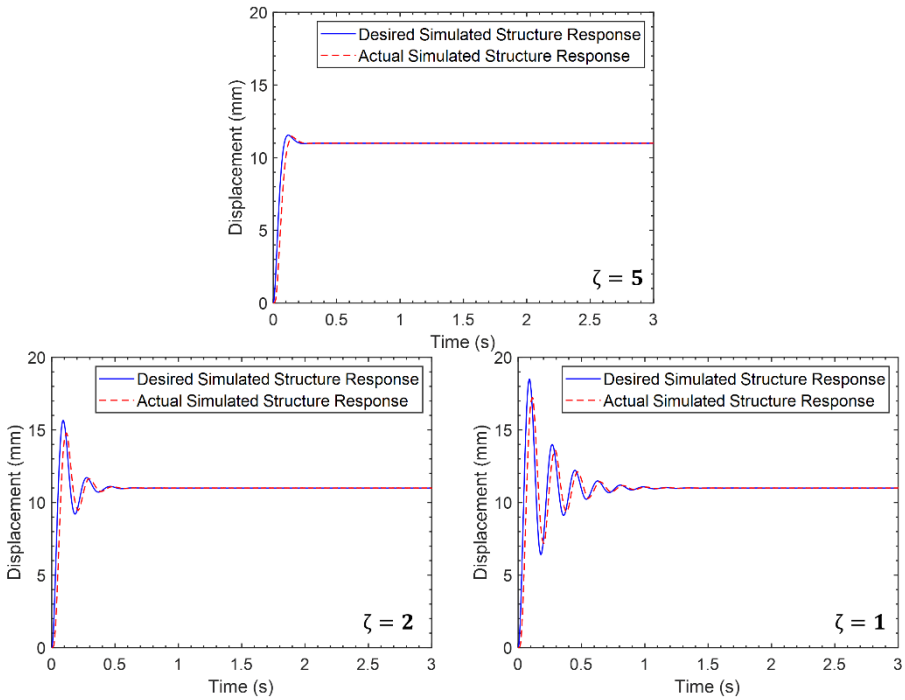

Figure 4. Desired simulated structure response and actual simulated structure response for Simulation 1, for a mass of 5 kg, stiffness of 125 N/m, and a damping ratio of 5 (top), 2 (bottom left), and 1 (bottom right).

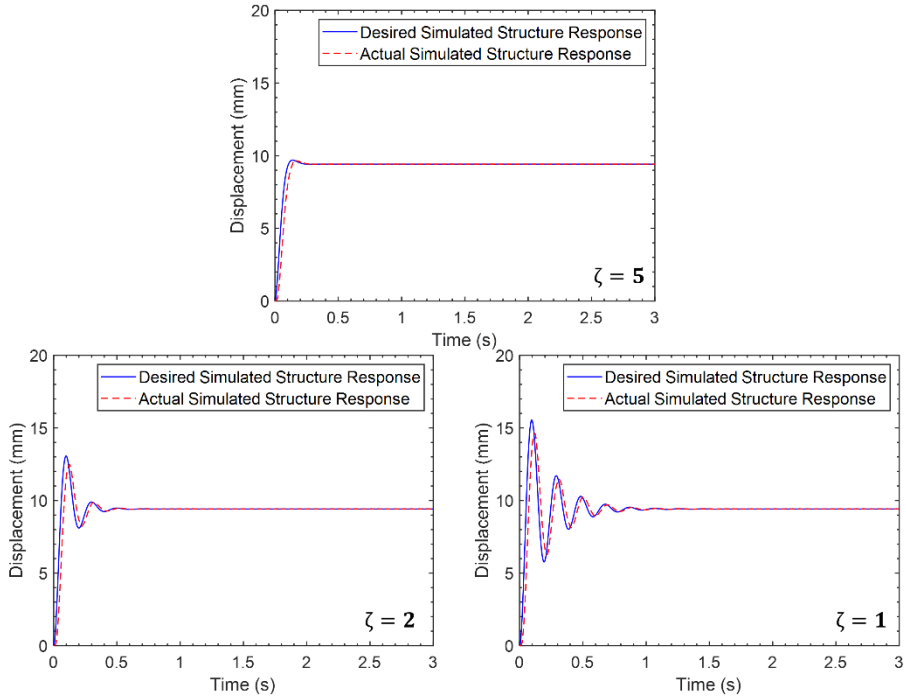

Figure 5. Desired simulated structure response and actual simulated structure response for Simulation 2, for a mass of 6 kg, stiffness of 150 N/m, and a damping ratio of 5 (top), 2 (bottom left), and 1 (bottom right).

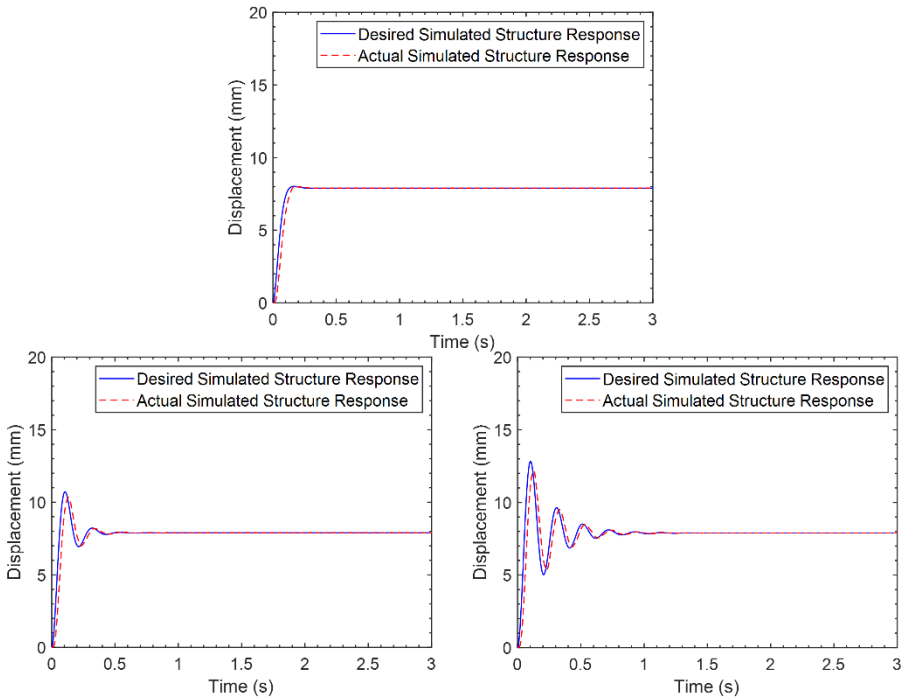

Figure 6. Desired simulated structure response and actual simulated structure response for Simulation 3, for a mass of 7 kg, stiffness of 175 N/m, and a damping ratio of 5 (top), 2 (bottom left), and 1 (bottom right).

From these simulated results, we observe that the PI controller for the HIL emulator can effectively emulate the desired mass-spring-damper response based on the FAM model and second-order ODE describing the dynamics of the mass-spring damper. There is some delay in the response of the controller, but this could be improved with a better-tuned controller. However, this only proves that the controller works with an analytical model of a hydraulic piston-cylinder. In order to truly determine the efficacy of this control strategy, it is necessary to see if the controller is effective in emulating a mass-spring-damper within actual hardware. In the subsequent section of this paper, we will demonstrate this through a proof-of-concept experiment.

4. EXPERIMENTAL PROOF-OF-CONCEPT FOR HIL EMULATOR

As shown analytically in the previous section, a simple PI controller can be used to program a hydraulic cylinder to behave with the dynamics of a desired structure (in this case, a mass-spring-damper). To prove that this concept is both valid and can be extended to experimental studies (and other analytical studies), we devised a simple experiment using the actual linear dynamometer hardware[13] to emulate multiple mass-spring-damper systems with different mass, stiffness, and damping properties. The experimental setup consists of a FAM attached to the linear dynamometer, with the load cell at the interface between the two to measure the force of the FAM on the drive cylinder. A picture of the experimental setup is shown in Figure 7. The FAM is pressurized at 206.84 kPa (30 psi), and the force exerted by the FAM on the drive cylinder, measured by the load cell, is used as an input to the HIL controller. Much like the simulation, a simple PI controller is used to control the cylinder itself.

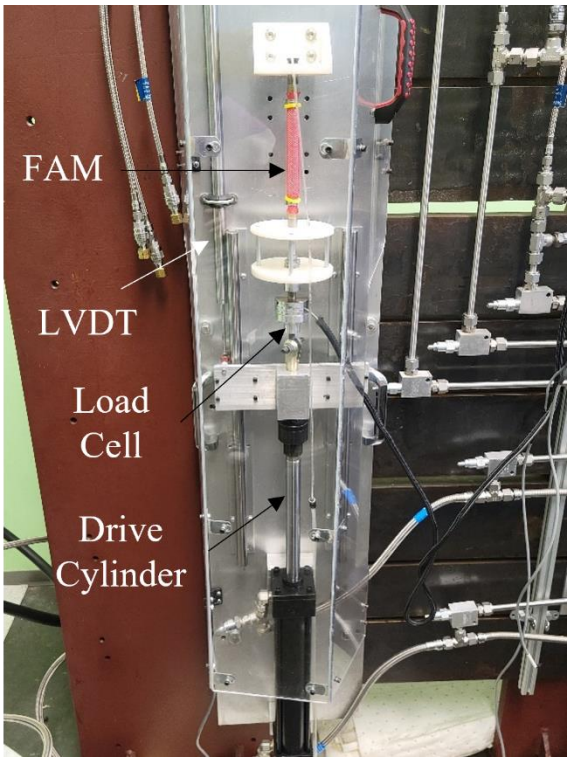

Figure 7. Hardware setup for experimental proof-of-concept of HIL emulator. Setup consists of a single FAM with a length of 0.127 m, an outer radius of 0.0127 m, and an inner radius of 0.0064 m, and an initial braid angle of 29.67 degrees. The FAM is pressurized pneumatically with an initial pressure of 206.84 kPa (30 psi).

The parameter sets tested in the experiments are shown in Table 2. Although the mass and stiffness parameters were kept the same as those in the simulations, the damping ratios were increased based on preliminary observations that the apparent damping in the actual system is lower than that of the simulation. Therefore, higher damping ratios were needed to ensure that that the overshoot in the system would stay within the physical bounds of the experiment. It is also important to note that the FAM parameters used in the simulation are based on an empirical model for a different FAM of different material and were chosen because of their availability, ease of implementation and simplicity. As a result, although the behavior of the FAM used in the experiment is similar, this FAM has different blocked force and free strain parameters than those of the FAM used in the model, making this experiment a qualitative, rather than a quantitative, validation.

Table 2. Desired mass, stiffness, and damping parameters used in proof-of-concept experiment.

Desired system parameters	**Test 1**	**Test 2**	**Test 3**
m_{des} (kg)	5	6	7
k_{des} (N/m)	125	150	175
ζ_1	25	25	25
ζ_2	20	20	20
ζ_3	15	15	15

The experimental results for each test case are shown in Figure 8, Figure 9, and Figure 10. In all cases, the actual response tracks the desired response well, with some delay in the response time, small steady-state error, and some minor bandwidth limitations. We believe that the bandwidth and delay issues can be rectified with better controller refinement. With regard to the steady-state tracking error and the fact that the response never quite settles down to zero, this is most likely due to noise in the load cell force measurements. Attempts to filter this noise would undoubtedly worsen the delay in the controller

response time. A tradeoff between controller response time and settling time based on the amount of noise filtering would be an interesting item for future study. Although the parameters of the actual drive cylinder (and the damping ratios, as previously discussed) are different from those used in the simulation, the experimental results qualitatively match the simulation results well, partially validating the model used for the drive cylinder and showing that the control algorithm is effective and justifying the use of the model in future simulations of other desired systems. Much like what was shown in the analytical simulations, although the natural frequency of the mass-spring-damper in each test case is held constant at 5 rad/s, the damped natural frequency of the emulated response increases as the desired mass/stiffness parameters decrease. This is because as the desired mass-spring-damper stiffness decreases, the FAM stiffness plays a more important role in the overall stiffness of the system, thus raising the damped natural frequency of the system. A summary of this trend is shown in Table 3.

Table 3. Damped natural frequency for two of the three effective damping ratios tested. The results for $\zeta = 25$ were difficult to obtain because it was so heavily damped.

m_{des}	$\omega_d\ (\zeta = 20)$	$\omega_d(\zeta = 15)$
5 kg	7.12 rad/s	8.36 rad/s
6 kg	5.85 rad/s	7.95 rad/s
7 kg	5.44 rad/s	7.54 rad/s

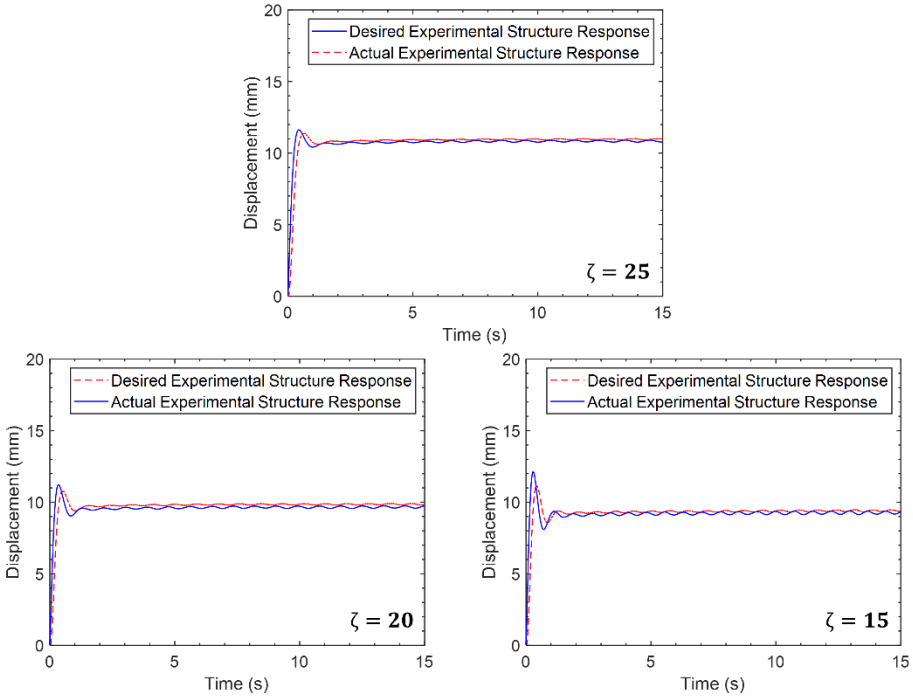

Figure 8. Experimental results for m = 5kg, k = 125 N/m, for damping ratios of 15, 20, and 25.

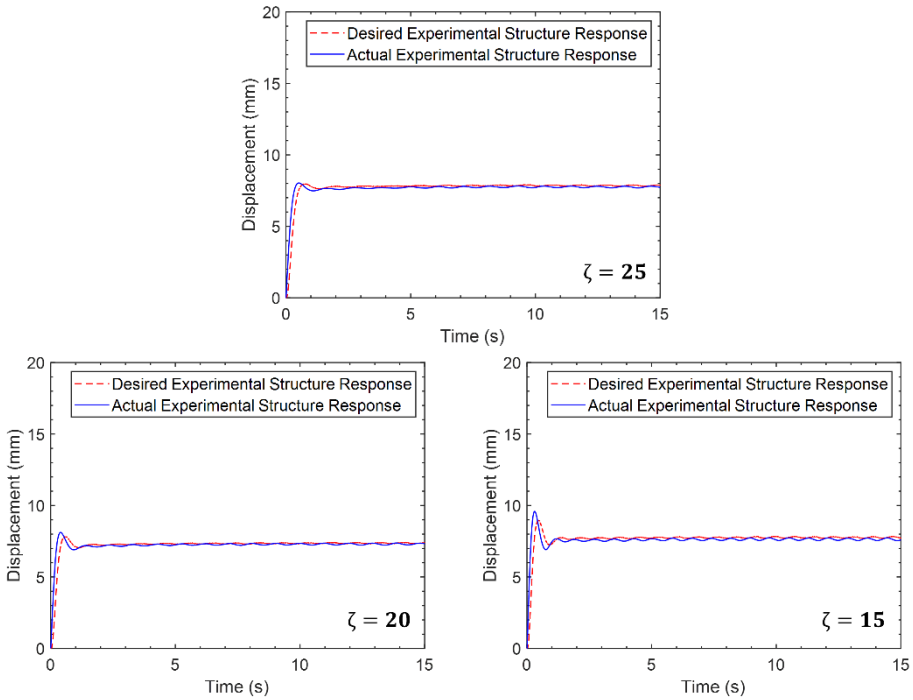

Figure 9. Experimental results for m = 6 kg, k = 150 N/m, for damping ratios of 15, 20, and 25.

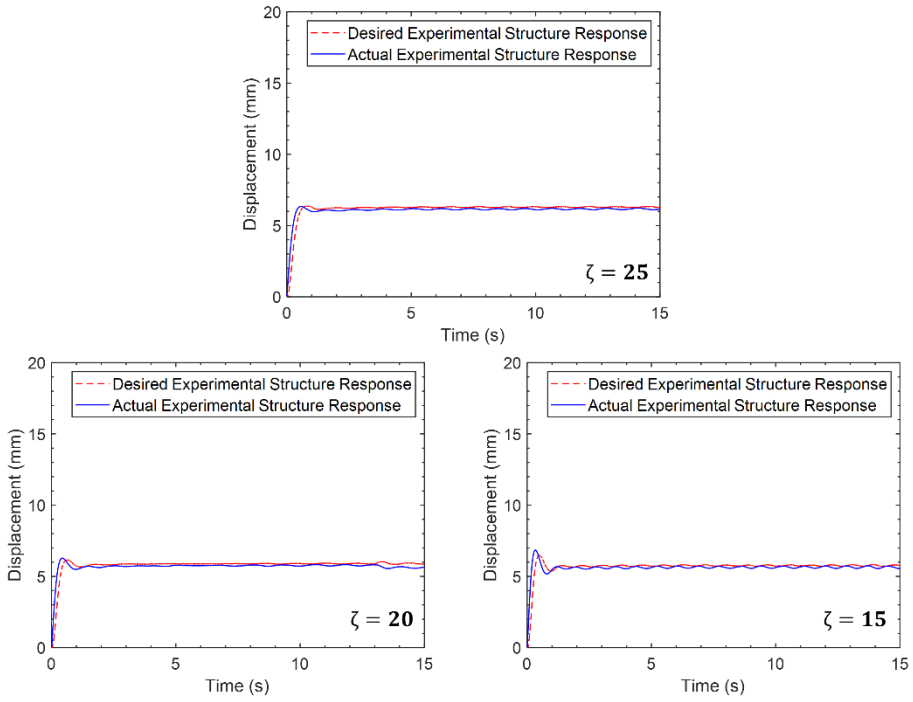

Figure 10. Experimental results for m = 7kg, k = 175 N/m, for damping ratios of 15, 20, and 25.

On the whole, the results of this proof-of-concept experiment demonstrate that the concept of using a linear hydraulic piston-cylinder as a HIL emulator to emulate the desired properties of a dynamic system works on both an analytical and

an experimental level. The FAM and the hydraulic cylinder used in the analytical section of this paper are not the same as the FAM and hydraulic cylinder used in the experimental section, but with a proper characterization of both, we believe that the analytical controller results would match very closely with the experimental results. Moving forward, this analytical framework will be used to develop controllers that can emulate much more complicated systems, such as a joint in a multi-DOF humanoid robotic arm. Based on the experimental results in this paper, once these controllers are developed, they can be analytically tested in Simulink and then validated using the actual hardware as a HIL emulator. In addition, the analytical and experimental frameworks can be used to incorporate bioinspired actuation strategies like variable recruitment.

5. CONCLUSIONS

In this paper, we analyzed a hardware-in-the-loop emulator that can be used to emulate the dynamics of a desired system. A model for the emulator, which is a linear dynamometer that uses a hydraulic drive cylinder, was developed using modeling tools from the literature. We then used this model to analytically demonstrate that a PI controller could be used to make the hydraulic cylinder emulate a mass-spring-damper actuated by a FAM at constant pressure. To demonstrate the validity of this control method, we then performed a proof-of-concept experiment using the linear hydraulic dynamometer first developed in 2017[13] (and since modified for improvements) and an actual FAM actuated at a constant pressure. The results of the experiment qualitatively demonstrate the validity of the analytical model used for the hydraulic cylinder, which will be used in the future to develop controllers to emulate more complicated robotic and bioinspired systems. The results of the experiment also show that the current hardware used for the linear dynamometer has the capabilities necessary to be a cyber-physical emulator for a wide range of parameters. Overall, this paper lays the foundation for future simulations and experiments involving the HIL emulator, fluidic artificial muscles, variable recruitment, and bioinspired robotics.

6. ACKNOWLEDGEMENTS

The authors gratefully acknowledge funding support for this research from the Faculty Early Career Development Program (CAREER) of the National Science Foundation under NSF Award Number 1845203 and Program Manager Irina Dolinskaya. Additionally, this material is based upon work supported by the National Science Foundation Graduate Research Fellowship Program under Grant No. 1650114. Any opinions, findings and conclusions or recommendations expressed in this material are those of the author(s) and do not necessarily reflect those of the National Science Foundation.

REFERENCES

[1] Fathy, H. K., Filipi, Z. S., Hagena, J. and Stein, J. L., "Review of hardware-in-the-loop simulation and its prospects in the automotive area," Modeling and simulation for military applications **6228**, 117–136, SPIE (2006).
[2] Bouscayrol, A., "Different types of hardware-in-the-loop simulation for electric drives," 2008 IEEE International Symposium on Industrial Electronics, 2146–2151, IEEE (2008).
[3] Mackowski, A. W. and Williamson, C. H., "Developing a cyber-physical fluid dynamics facility for fluid–structure interaction studies," Journal of Fluids and Structures **27**(5–6), 748–757 (2011).
[4] Waghela, R., Bryant, M. and Wu, F., "Control design in cyber-physical fluid–structure interaction experiments," Journal of Fluids and Structures **82**, 86–100 (2018).
[5] Tondu, B., "Modelling of the McKibben artificial muscle: A review," Journal of Intelligent Material Systems and Structures **23**(3), 225–253 (2012).
[6] Kang, B.-S., Kothera, C. S., Woods, B. K. and Wereley, N. M., "Dynamic modeling of Mckibben pneumatic artificial muscles for antagonistic actuation," 2009 IEEE International Conference on Robotics and Automation, 182–187, IEEE (2009).

[7] Tondu, B., Ippolito, S., Guiochet, J. and Daidie, A., "A seven-degrees-of-freedom robot-arm driven by pneumatic artificial muscles for humanoid robots," The International Journal of Robotics Research **24**(4), 257–274 (2005).
[8] Bryant, M., Meller, M. A. and Garcia, E., "Variable recruitment fluidic artificial muscles: modeling and experiments," Smart Materials and Structures **23**(7), 074009 (2014).
[9] Henneman, E., Somjen, G. and Carpenter, D. O., "Excitability and inhibitibility of motoneurons of different sizes," Journal of neurophysiology **28**(3), 599–620 (1965).
[10] Chapman, E. M., Jenkins, T. and Bryant, M., "Design and analysis of electrohydraulic pressure systems for variable recruitment in fluidic artificial muscles," Smart Materials and Structures **27**(10), 105024 (2018).
[11] Jenkins, T. E., Chapman, E. M. and Bryant, M., "Bio-inspired online variable recruitment control of fluidic artificial muscles," Smart Materials and Structures **25**(12), 125016 (2016).
[12] Meller, M., Chipka, J., Volkov, A., Bryant, M. and Garcia, E., "Improving actuation efficiency through variable recruitment hydraulic McKibben muscles: modeling, orderly recruitment control, and experiments," Bioinspiration & biomimetics **11**(6), 065004 (2016).
[13] Chipka, J., Meller, M. A., Volkov, A., Bryant, M. and Garcia, E., "Linear dynamometer testing of hydraulic artificial muscles with variable recruitment," Journal of Intelligent Material Systems and Structures **28**(15), 2051–2063 (2017).
[14] Ruderman, M., "Full- and reduced-order model of hydraulic cylinder for motion control," IECON 2017 - 43rd Annual Conference of the IEEE Industrial Electronics Society, 7275–7280, IEEE, Beijing (2017).
[15] Jelali, M. and Kroll, A., [Hydraulic servo-systems: modelling, identification and control], Springer Science & Business Media (2012).
[16] Meller, M., Kogan, B., Bryant, M. and Garcia, E., "Model-based feedforward and cascade control of hydraulic McKibben muscles," Sensors and Actuators A: Physical **275**, 88–98 (2018).
[17] Meller, M. A., Bryant, M. and Garcia, E., "Reconsidering the McKibben muscle: Energetics, operating fluid, and bladder material," Journal of Intelligent Material Systems and Structures **25**(18), 2276–2293 (2014).